Effect of Channel Dimensions on Micro PEM Fuel Cell Performance Using 3D Modeling

P.Ramesh*‡, S.P. Duttagupta*

*Department of Electrical Engineering,IIT Bombay

ramp@ee.iitb.ac.in, sdgupta@ee.ittb.ac.in

‡ Corresponding Author; P.Ramesh, Department of Electrical Engineering ,IIT Bombay, Mumbai ,Maharashtra, 400076, 00919496370467, ramp@ee.iitb.ac.in

Received: 20.02.2013 Accepted: 04.04.2013

Abstract- Proton exchange membrane fuel cells are electrochemical devices, which are emerging as promising power sources for portable electronic applications. One of the key component of the fuel cell is the flow channel. The flow channel ensures uniform distribution of the fuel and oxygen to the reaction sites. If the distribution is non uniform, it will affect the performance of the fuel cell. The width of the channel and the rib plays a significant role in uniform fuel distribution . Here we build a three dimensional model for a fuel cell using COMSOL Multiphysics. The performance of the cell is studied under varying channel widths and rib widths.

Keywords- PEM Fuel cell, 3-D modeling, Gas Diffusion layer, Membrane Electrode Assembly.

1. Introduction

Fuel cells [1] are emerging as the power sources of the future. PEM fuel cell [2] are the most popular type of fuel cells which use hydrogen as the fuel. The necessary improvements for fuel cell operation [3] and performance demands better design and optimization. These issues can be addressed easily if mathematical models [7][9][10] are available. Traditionally the flow field plates are made of graphite and the current collection is carried out from the flow field plates. But in literature, many authors [4][5][6] have reported building micro fuel cells, where the flow field plates are also made of silicon. The channel width and rib width plays an important role in the performance of micro fuel cells. Rib width is defined as the width of the GDL which is not covered by the flow channel.

Various researchers have performed simulation studies [12,13] on the effects of flow-channel geometric parameters on cells with varying channel dimensions. Palaniappan etal [26] investigated the effect of mal flow distribution in PEM fuel cells and reported performance loss as a result of non uniform fuel distribution across the reaction sites. Scholta et al [23] predicted that narrow channels are preferable for high current densities, whereas wider channels are favored at low current densities. Shimpalee et al [20,24] showed that the flow-channel path length and other channel geometric dimensions affect cell performance .They also found that too deep channel depth tend to reduce the local gas pressure, leading to variances in fuel distributions. Wang et al [21] build a numerical model for a PEM fuel cell with serpentine channels and studies the effect of channel dimensions. Kumar et al [18] studied the effect of channel dimensions and shape on pem fuel cell performance .The studies by Feng et al [13] revealed that the performance of a PEMFC with a serpentine flow channel is insensitive to channel depth in certain operation conditions. Investigations by Manso et al [25] on the effects of the aspect ratio (defined as the ratio of channel depth to width) on the performance of miniature cell indicated that cells with a high aspect ratio yield higher current densities. This result differs from other simulation results, in which channel depth had no significant effects [22,23]. This disagreement may result from the differences in channel scales. Deeper channel depths provide sufficient space for reactant transportation and water removal. However, it also enlarges the channel cross-sectional area and slow down flow velocity, which subsequently affects mass transfer rate and water balance in the membrane electrode assembly Although numerous papers [12,15,16,17] explore flow channel geometric variables using two dimensional simulation , only a few papers [8,13,14,19] have dealt with three dimensional simulation, especially in

miniature scale. It is more challenging to implement a three dimensional fuel cell model and examine the effects of flow-channel geometric parameters on efficient miniature fuel cells

2. Governing Equations for the Fuel Cell Model

The gas flow within the channel is assumed to take place by convection and diffusion .The gas flow in the gas channel is modeled with the momentum and continuity equations (the Navier-Stokes equations):

$$\frac{\partial(\varepsilon\rho u)}{\partial t}+\nabla.(\varepsilon\rho uu)=-\varepsilon\Delta p+\nabla.(\varepsilon\mu^{eff}\Delta u)+S_u \quad (1)$$

$$\frac{\partial(\rho\varepsilon)}{\partial t}+\nabla.(\varepsilon\rho u)=0 \quad (2)$$

where ε is the porosity ,μ the dynamic viscosity, (Pa.s),

ρ the density (Kg/m^3),S_u is the source term (for any external force),p is pressure (Pa),u – gas velocity vector (m/s).

Navier Stokes equations are applied in the gas channel with source term equal to zero while it is added as Darcy law in the GDL and catalyst layer to describe the flow in the porous media (Darcy law) along with the viscous effects that are important at the boundary between flow channel and GDL.

The mass flux in the gas phase is based on the Maxwell-Stefan diffusion and convection equations. It is described by this expression for species j:

$$\nabla.(\rho X_i u)=\nabla.(\rho\sum_{j=1}^{n-1}D_{ij}^{eff}\nabla X_j)+S_i \quad (3)$$

Where D_{ij}^{eff} is the effective diffusion constant.

Since gas diffusion layers (GDL) and catalyst layers are porous media, the velocity distribution is therefore formulated by Darcy's law and mass conservation equation.

Darcy's Law:

$$u=-\frac{\kappa}{\mu}\nabla P \quad (4)$$

where κ is the permeability, m^2; and μ the dynamic viscosity, Pa.s;

The continuity of current in a conducting material is described by

$$\nabla.i=0 \quad (5)$$

In a PEM fuel cell, the conducting materials are porous electrodes and membrane. The current is therefore split into two parts: the ionic current and the electronic current. Protons travel through the ionic conductor (the membrane) to form an ionic current denoted by i_e, while electrons can only be transferred through the solid matrix of electrodes which results in an electronic current denoted by i_s. The continuity equation of current then becomes:

$$\nabla.i=\nabla.i_s+\nabla.i_e 0 \quad (6)$$

In the catalyst layer, where a chemical reaction occurs on a three-phase boundary, electrons are either transferred from the solid matrix to electrolyte or vice versa. This two-way transfer of electrons between solid matrix and electrolyte makes the transfer current density, denoted by j, a source term in one phase, and a sink term in the other phase. The potential equations for both solid and electrolyte phases are obtained by applying Ohm's law to Eq. (12).

Electron transport

$$\nabla.(\sigma_s^{eff}\nabla\phi_s)+S_{\phi s}=0 \quad (7)$$

Proton transport

$$\nabla.(\sigma_m^{eff}\nabla\phi_m)+S_{\phi e}=0 \quad (8)$$

Where ϕ is the phase potential, σ_m^{eff} is the effective electric conductivity or also can be termed as the ionic conductivity in the membrane given by S/m; σ_s^{eff} is the effective electrode conductivity,

S the current source term, A/m^3; the subscript s denotes the property of a solid phase and e denotes that of an electrolyte phase. The source terms in the electron and proton transport equations, i.e., Eq. (13-14), result from the electrochemical reaction occurring in the catalyst layers of anode and cathode sides. The effective conductivity σ_m^{eff} is given by

$$\sigma_m^{eff}=\varphi_m^{1.5}e^{1268\left(\frac{1}{303}-\frac{1}{T}\right)}.(0.5139\lambda-0.326)\ ;\lambda>1 \quad (9)$$

$$\sigma_m^{eff}=\varphi_m^{1.5}e^{1268\left(\frac{1}{303}-\frac{1}{T}\right)}(0.1879)\ \text{ for }\ \lambda\le 1$$

Where φ_m - Volumetric fraction of ionomer in the catalyst layer, T is absolute temperature in Kelvin,

λ is the water content in the membrane phase which is related to the activity of water vapor in the adjacent pores, given by $a=\chi_{H2O}\frac{P}{P_{sat}}$,P is the gas pressure, P_{sat} is the saturation gas pressure, χ_{H2O} is the gas phase water mass fraction)

Using an experimentally derived relationship by Springer for Nafion 117 membrane

$\lambda=0.043+17.81a-39.85a^2+36a^3$ for $0\le a\le 1$ (10)

$\lambda=14+1.4(a-1)$ for $a>1$

The source terms are

Anode catalyst layer and Cathode catalyst layer

$$S_{\phi s}=-j_a S_{\phi s}=-j_c \quad (11)$$

$$S_{\phi e}=j_a S_{\phi s}=j_c \quad (12)$$

Where j_a and j_c are the transfer current density corresponding to the electrochemical reaction at the anode

and cathode catalyst layers. The transfer current densities are given by Butler-Volmer equations

$$j_a = Aj_{0,a}^{ref}\left(\frac{C_{H2}}{C_{H2}^{ref}}\right)\left(e^{-\alpha_{c,a}\eta_a F/RT} - e^{\alpha_{a,a}\eta_a F/RT}\right) \quad (13)$$

$$j_c = Aj_{0,c}^{ref}\left(\frac{C_{O2}}{C_{O2}^{ref}}\right)\left(e^{-\alpha_{c,c}\eta_a F/RT} - e^{\alpha_{a,c}\eta_a F/RT}\right) \quad (14)$$

A – electrode active surface area in m^2
η – activation overpotential
F – Faraday's constant
R – universal gas constant
T- absolute temperature in Kelvin
j_0 – exchange current density A/m^2

3. Experimental

The Nafion 212 membrane was boiled in 3% H_2O_2 solution for 1 hour. Then membrane was placed in deionized water and boiled for 1 hour. Again membrane was boiled in 0.5 M H_2SO_4 solution and again boiled in deionized water. The membrane is ready for use now. Two pieces of Toray carbon paper were cut in size of 2.2cm x 2.2cm.Amorphous carbon Vulcan XC- 72 of weight was ultra sonicated in isopropanol to which PTFE dispersion was added, which varies from 15 to 30 wt% to make the slurry. This slurry was then brushed on carbon paper pieces and dried at 80^o C to make GDL.The above steps were repeated with platinized carbon from E-Tek. 20% weight of platinum on carbon. Nafion concentration was kept fixed at 30 wt % of catalyst. Platinum loading was 0.2 mg/ cm^2 on anode and 0.4 mg / cm^2 on cathode. Now the two electrodes are ready and placed the membrane in between the two electrodes, which was sandwiched between 2mm thick Teflon sheets and hot pressed the assembly together for 2 min under 50 atm of pressure, at approx 125 degrees.

The MEA is tested in Arbin Instruments fuel cell test station with 100 % humidified oxygen and hydrogen gas. Flow rates were maintained at 0.2 SLPM. The gas was passed for 15 min to completely humidify the membrane after which a constant current was drawn in the intervals of five minutes and voltage is noted. Impedance spectroscopy was performed in galvanostatic mode for current densities upto 1.2 A/cm^2 where anode is used as a reference and counter electrode whereas cathode served as a working electrode.

4. The Model

A 3 dimensional model[8] of a PEM fuel cell is implemented using COMSOL Multiphysics. The present model is established based on the following assumptions:

- Flow is laminar everywhere due to small gas pressure gradient.
- Reactant gases behave as the ideal gas mixture.
- The electrodes and membrane are made of homogeneous materials.
- The temperature distribution across the cell is uniform.
- Water exists only in the gas phase in the fuel cell.
- The polymer electrolyte membrane is impermeable to reactant gases.
- Protons can only transport through the electrolyte, and electrons through the solid phase.
- Three species including oxygen, water and nitrogen are considered on the cathode side while only hydrogen and water are considered on the anode side.
- The fuel cell is operating at the steady state.

Figure 1 shows the structure of the model developed in Comsol Multiphysics. The top part is the anode side while bottom part corresponds to the cathode. The operating conditions and parameters of the model are given in Table 1.

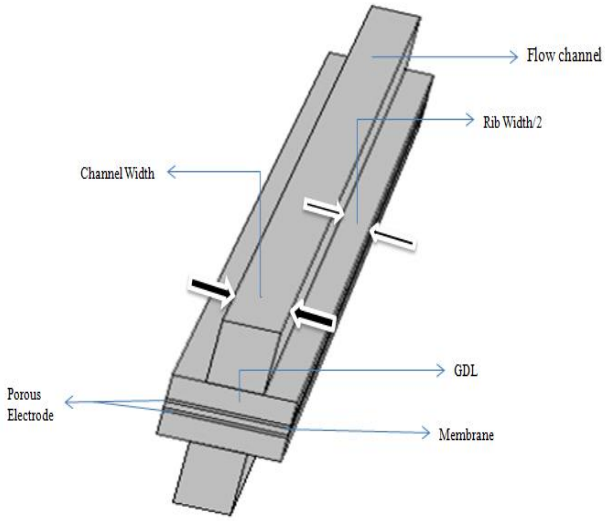

Fig. 1. The schematic PEM fuel cell model

Table 1. Operating conditions of the model

Cell length (L)	1mm
Channel height	1mm
Channel width	0.7mm
Rib width	1mm
GDL width	0.3 mm
Porous electrode thickness	0.5 mm
Membrane thickness	0.05 mm
GDL Porosity	0.4
GDL electric conductivity	1000 S/m
Inlet H_2 mass fraction (anode)	0.743
Inlet H_2O mass fraction (cathode)	0.023
Inlet oxygen mass fraction (cathode)	0.228
Anode inlet flow velocity	0.2m/s
Cathode inlet flow velocity	0.5m/s
Anode viscosity	1.19 E-5 Pa.s
Cathode viscosity	2.46 E -5 Pa.s
Permeability (porous electrode)	2.36 E -12 m^2
Membrane conductivity	10 S/m

5. Result

Figure 2 shows the experimental and modeled polarization plot. Fitting is obtained by varying active surface area of the catalyst per unit volume and cathodic Tafel slope. Membrane conductivity was determined from the high frequency intercept in the Nyquist plot, assuming negligible contact resistance. Its estimated value is 10 S/m over the modeled current density range.

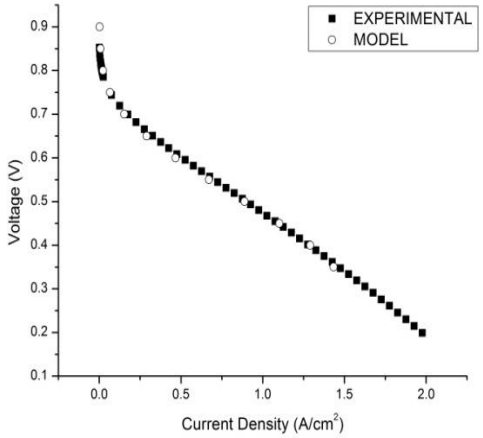

Fig. 2. Polarization plot for experimental and modelling results

Impedance spectroscopy in Fig 3 shows the Nyquist plot for the MEA. Following observations can be made from these plots.

1. For all current densities HFR is nearly the same which means no change in membrane conductivity. But there is slight increase in HFR above current density of 1 A/cm^2, which may be due to gradient of water across the membrane due to higher production rate of water at the cathode.

2. Mid frequency arc diminishes as current density increases. This is due to decrease in charge transfer resistance which is related to the faster kinetics of oxygen reduction at high current densities. This behavior is observed upto current density of 1.2 A/cm^2, the mid frequency arc starts increasing after this. This may be attributed to oxygen mass transport limitations due to water accumulation on the cathode side.

3. The low frequency arc of small diameter appears above the current density of 1.5 A/cm^2, which is attributed to the start of flooding in the electrode due to liquid water accumulation.

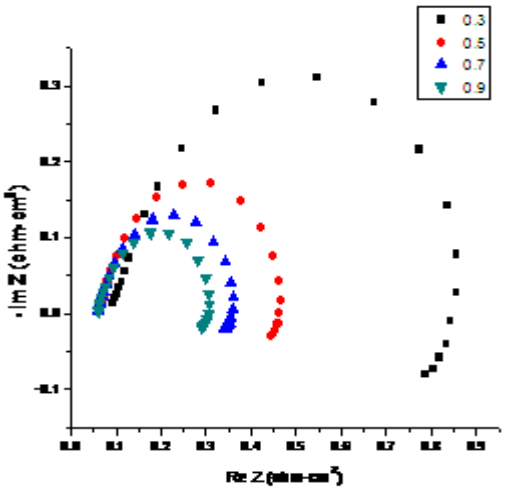

Fig. 3. Nyquist plots of the mea, values assigned to the markers refers to the total current

6. Effect of Channel Width

Effect of channel width on the performance of the cell is studied by varying the width of the channel and keeping channel width to rib ratio constant at 1. All other parameters of the cell are kept constant. As can be seen from the Figure 4 that the performance of the cell degraded as the width of the channel is increased from 0.5 mm to 2 mm. The probable reason for this stems from oxygen concentration distribution in the cell for various channel widths as oxygen concentration is directly related to local current density inside the cell at higher current densities.

Figure 5 shows oxygen mole fraction on the surface of cathode catalyst layer along the length of the channel. These line graphs are taken at the center of the length of the cell. From these profiles it appears to contradict the assumption mentioned above as the oxygen fraction is highest for the channel width of 2 mm and lowest for the channel width of 0.5 mm. But the situation becomes clearer when we look at Figure 6. It shows oxygen mole fraction plotted in the direction perpendicular to the channel on the catalyst surface. Gaussian distribution of the species is observed with the peak in the middle of the channel. It includes the effect of the rib where the catalyst underneath the rib is hidden. From the Figure 5, it is clear that oxygen mole fraction is increased under the rib as the width of the channel is decreased. This is due the higher pressure drops created along the length of the channel at smaller widths of the channel. This scenario is clear from the Figure 7 which shows the pressure of the mixture along the length of the channel. Higher pressure drop forces more oxygen molecules inside the rib thereby increasing their concentration.

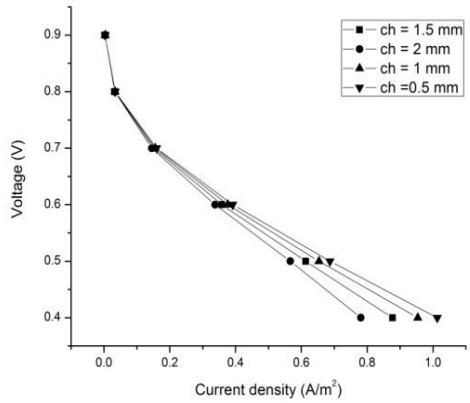

Fig. 4. Polarization curves for different channel widths with channel width to rib width ratio is one

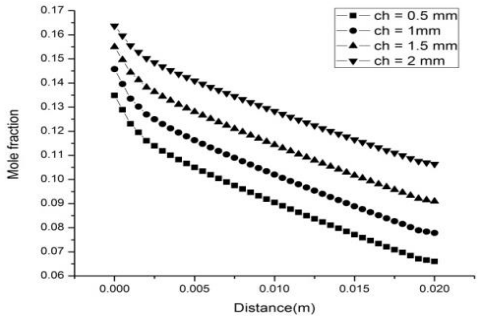

Fig. 5. Oxygen mole fraction along the length of the channel for different channel widths at cell potential of 0.4 V

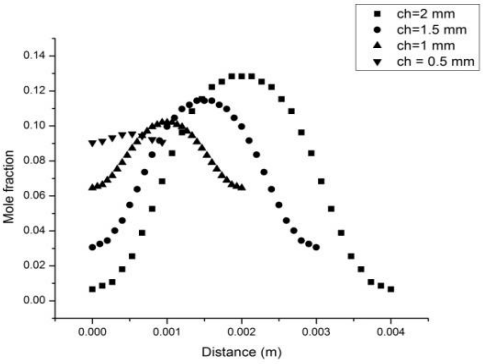

Fig. 6. Oxygen concentration profiles across the length of the channel for different channel widths at cell potential of 0.4 V

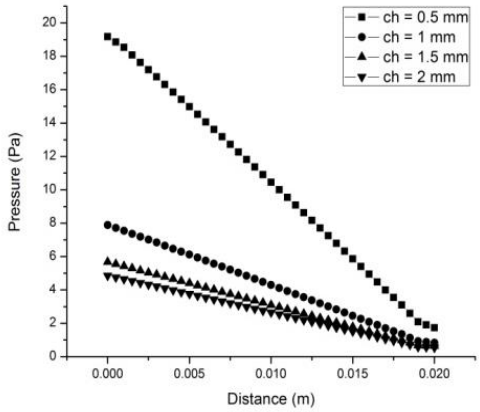

Fig. 7. Pressure variation along the length of the channel for different channel widths

7. Effect of Rib Width

Figure 8 shows the simulated polarization curves for the constant channel width and varying channel rib. As expected the performance of the cell is lowered as the width of the rib is increased because of the oxygen mole fraction distribution as shown in Figure 9. But the performance degradation is higher beyond rib width of 0.7 mm. Cells with rib widths of 0.2 and 0.7 have nearly the same performance.

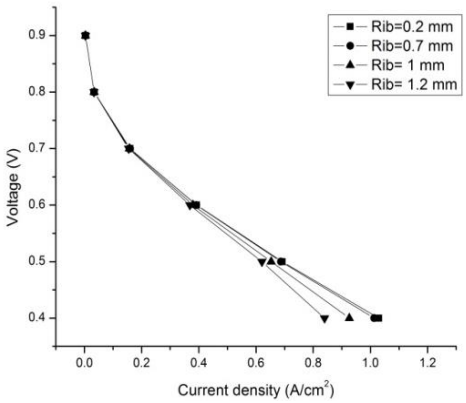

Fig. 8. Polarization curves for different rib widths with channel width kept constant at 0.5

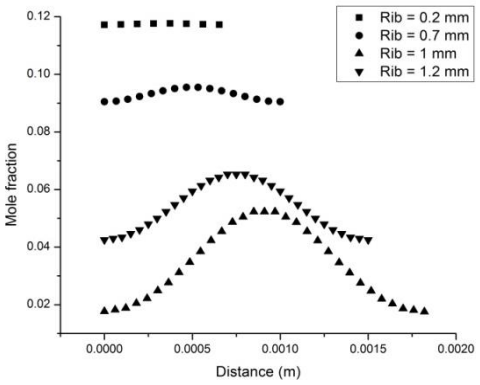

Fig. 9. Oxygen mole fraction profiles across the length of the channel for different rib widths for cell potential of 0.4 V

8. Conclusion

A 3-dimensional model for PEM fuel cell is validated under the experimentally feasible assumptions. The effect of channel width and rib width on the fuel cell performance is studied by considering various channel widths and rib widths employing different distributions and dimensions. The performance of the cell is degraded as the width of the channel is increased from 0.5 mm to 2 mm. The performance of the cell is lowered as the width of the rib is increased. But decreasing the channel width and rib width below a threshold value can affect the fuel transfer along the channel and hence affect the cell performance. So there exists an optimum value of channel. width and rib width for which the fuel cell will give better performance. Experimental study has to be performed with various channel and rib widths so as to validate the simulation results.

References

[1] B Viswanathan, M Aulice Scibioh. "FUEL CELLS Principles and applications." Chennai: University Press , 2006,ch.2.

[2] Ryan O Hayre, Suk Won Cha,Whitney Collela,Fritz B Prinz. "Fuel Cell Fundamentals. New york: John Wiley and sons, 2005,ch .4.

[3] T.S.Zhao, K.D Kreur .Trung Van Nguyen. "Advances in Fuel cells." Great Britain: Elsevier, 2007, ch. 3.

[4] C.Xie, J.Bostaph,J.Pavio. "Development of a 2W direct methanol fuel cell power source." Journal of power sources , Vol 136, pp. 55-65, 2004.

[5] Zhen Guoa, Amir Faghri. "Development of planar air breathing direct methanol fuel cell stacks." Journal of power sources. Vol 160 ,pp. 1183- 1194, 2006.

[6] Stefan Wagner Roger Hahn, H. R. "Development of Micro Fuel cells with MEMS". MINATEC , 2003.

[7] Adrew Rowe, Xianguo Li. "Mathematical modeling of proton exchange membrane fuel cells." Journal of power sources, pp. 82-96,2001.

[8] S Dutta, S Shimpalee ,J W Van Zee. "Three Dimensional numerical simulation of straight channel PEM Fuel Cells." Journal of Applied Elecrochemistry , pp. 135-146, 2000.

[9] Sukkee Um, C Y Wang , K S Chen. "Computational Fluid Dynamics Modelling of Proton Exchange Membrane Fuel Cells." Journal of the Electrochemical society ,pp.4485- 4493,2000.

[10] Vladimir Gurau, Hongtan Liu, Sadik Kakac, "Two Dimensional model for proton exchange membrane fuel cells." AIChE Journal, pp. 2410- 2422, 2000.

[11] Arico A. S., Cretì P., Baglio V.,Modica, E.Antonucci, ,"Influence of flow field design on the performance of a direct methanol fuel cell", Journal of Power Sources, Vol 91, pp 202- 209,2000.

[12] Choi K. S., Kim H. M., Moon S.M." Numerical studies on the geometrical characterization of serpentine flow-field for efficient PEMFC", International Journal of Hydrogen Energy, Vol 36, pp. 1613-27, 2001.

[13] Ferng Y. M, Su A." A three-dimensional full-cell CFD model used to investigate the effects of different flow channel designs on PEMFC performance", International Journal of Hydrogen Energy, Vol 32,pp 4466-76,2007.

[14] Higier A., Liu H, "Optimization of PEM fuel cell flow field via local current density measurement,"International Journal of Hydrogen Energy, Vol 35, pp 2144-50,2012.

[15] Hsieh S.S., Chu, K. M,"Channel and rib geometric scale effects of flow field plates on the performance and transient thermal behavior of a micro-PEM fuel cell", Journal of Power Sources, Vol 173,pp 222-32,2007.

[16] Inoue, G., Matsukuma Y., Minemoto M, "Effect of gas channel depth on current density distribution of polymer electrolyte fuel cell by numerical analysis including gas flow through gas diffusion layer", Journal of Power Sources, Vol 157,pp 136-152,2006.

[17] Jeon, D. H., Greenway S., Shimpalee S., Van Zee J. W. ,"The effect of serpentine flow-field designs on PEM fuel cell performance".International Journal of Hydrogen Energy, Vol 33,pp 1052-1066,2008.

[18] Kumar A., Reddy R. G," Effect of channel dimensions and shape in the flow-field distributor on the performance of polymer electrolyte membrane fuel cells", Journal of Power Sources, Vol 113,pp 11-18,2003.

[19] Lobato J., Cañizares P., Rodrigo M.A., Pinar F. J., Mena E., Úbeda ," Three-dimensional model of a 50 cm2 high temperature PEM fuel cell.Study of the flow channel geometry influence". International Journal of Hydrogen Energy, Vol 35, pp 5510-20,2010.

[20] Shimpalee S., Van Zee J. W, "Numerical studies on rib and channel dimension of flow-field on PEMFC performance", International Journal of Hydrogen Energy, Vol 32, pp 842- 856,2007.

[21] Wang X. D., Yan W. M, Duan Y. Y., Weng F. B., Jung G. B., Lee C. Y.," Numerical study on channel size effect for proton exchange membrane fuel cell with serpentine flow field", Energy Conversion and Management , Vol 51,pp 959-68,2010.

[22] Yoon Y. G., Lee W. Y., Park G. G, Yang T. H.,Kim C. S," Effects of channel configurations of flow field plates on the performance of a PEMFC", Electrochemica Acta, Vol 50, pp709- 712,2004.

[23] Scholta J., Escher G., Zhang W., Küppers L.,Jorissen L., Lehnert W, "Investigation on the influence of channel geometries on PEMFC performance", Journal of Power Sources,Vol 155,pp. 66-71,2006.

[24] Shimpalee S., Greenway S., Van Zee J. W,"The impact of channel path length on PEMFC flow field design", Journal of Power Sources, Vol 160, pp 398-406,2006.

[25] Manso A. P., Marzo F. F., Mujika M.G., Barranco J., Lorenzo A," Numerical analysis of the influence of the channel cross-section aspect ratio on the performance of a PEM fuel cell with serpentine flow field design", International Journal of Hydrogen Energy, Vol 36,pp 6795- 6808,2011.

[26] K.Palaniappan, R.Govindarasu,R.Parthiban," Investigation of Flow Mal-distribution in Proton Exchange Membrane Fuel Cell Stack ",International Journal of Renewable Energy Research,Vol 2,No.4,2012.